https://doi.org/10.48048/tis.2025.8822

Physicochemical and Structural Properties of Resistant Starch Prepared from Tacca Tuber Starch using Autoclaving-Cooling and Acid Hydrolysis Treatments

Diode Yonata[1,2], Priyanto Triwitono[1], Lily Arsanti Lestari[3] and Yudi Pranoto[1,*]

[1]Department of Food and Agricultural Product Technology, Faculty of Agricultural Technology, Universitas Gadjah Mada, Yogyakarta, 55281, Indonesia
[2]Department of Food Technology, Faculty of Science and Agricultural Technology, Universitas Muhammadiyah Semarang, Semarang, 50273, Indonesia
[3]Department of Nutrition and Health, Faculty of Medicine, Public Health and Nursing, Universitas Gadjah Mada, Yogyakarta, 55281, Indonesia

([*]Corresponding author's e-mail: pranoto@ugm.ac.id)

Received: 9 August 2024, Revised: 21 August 2024, Accepted: 27 August 2024, Published: 15 November 2024

Abstract

Tacca tuber (*Tacca leontopetaloides*) is a neglected and underutilized plant species. Recently, tacca tuber has been studied as a food plant source of high-amylose starch, so it has the potential to be developed into resistant starch (RS), especially type-3 RS (RS3). RS3 can be prepared through the autoclave-cooling (AC) process, but the RS produced is not optimal. Further increase in RS can be obtained through hydrolysis of citric acid (AH). Until now, systematic knowledge about the preparation method and characterization of RS3 produced from tacca tuber starch through the AC-AH process remains unavailable. This study aims to determine the physicochemical properties and structure of RS3 from tacca tuber starch made through the AC-AH process. Tacca tubers were obtained from the Garut coast, Indonesia. They were first extracted to obtain starch and then processed using the AC process to make RS3. The acquired RS3 was hydrolyzed using AH at various concentrations and hydrolysis times. The results showed that all treatments did not affect the proximate composition, except for water content. Significant effects were observed on amylose and RS levels. The swelling power, solubility, water holding capacity, oil holding capacity and color profile of RS3 also significantly changed. The morphology of RS3 was deformed, accompanied by a change in its crystal structure to a combination of B and V types. This alteration was followed by an increase in the relative crystallinity and thermal profile, while the paste profile decreased significantly. In conclusion, all preparation methods affected the physicochemical properties and structure of RS3 from yam starch, except for the proximate composition. AC-AH treatment with 0.3 M citric acid for 4 h is recommended for preparing RS3 because it produces the highest RS content. The acquired RS3 has the potential to be applied in products that require good paste stability, and have health benefits.

Keywords: Tacca tuber starch, Resistant starch, Autoclaving-cooling, Acid hydrolysis, Citric acid, Physicochemical properties, Structural properties

Introduction

Tacca (*Tacca leontopetaloides*) is a tropical tuber plant classified as a neglected and underutilized plant species. This plant comes from Southeast Asia, mainly grows in the wild and can be found on coasts at an altitude of up to 300 m above sea level [1]. Starch is the main component of tacca tubers, which accounts for

32.43 % of fresh tubers or around 83.24 % of their dry weight [2]. Currently, the use of tacca tuber starch in the industry requires futher improvement. Tacca tuber starch has a high amylose content (32.81 - 35.25 %) and low crystallinity value (24.22 - 27.03 %), resulting in poor thermal properties and swelling properties [3]. Therefore, tacca tuber starch readily undergoes retrogradation [4].

Retrogradation is necessary to produce resistant starch (RS), especially type-3 RS (RS3). RS3 has good thermal stability. In addition, the RS3 production process is controlled, has a low cost, is energy efficient, and has a solid resistance to digestive enzyme hydrolysis [5,6]. Apart from that, consuming foods rich in RS is highly recommended because it offers various health benefits. This is because RS produces very few calories and is classified as a food with a low glycemic index [7,8]. Autoclave-Cooling (AC) is 1 method of making RS3. The autoclave process involves heating starch in excess water. Hot steam and high-pressure during autoclaving cause the starch's crystalline structure and amorphous areas to be damaged until the starch undergoes gelatinization. The cooling process causes the degraded starch molecules to re-associate to form a solid structure stabilized by hydrogen bonds [9,10]. The RS3 acquired by the AC method generally increases with the number of cycles [11-13]. However, recent research concluded that 2 cycles of AC treatment are recommended to obtain the highest levels of RS3 from tacca tuber starch [14].

Besides amylose, the amylopectin component can also contribute to the formation of RS through the acid hydrolysis (AH) treatment. The AH treatment cleaves the branched chains of amylopectin to produce straight-chain amylodextrin with a shorter chain length and lower molecular weight, and the process contributes to the increase in RS [15]. Based on existing research, amylopectin hydrolysis can be carried out before the AC treatment (AH-AC) or after the AC treatment (AC-AH). Most studies report that amylopectin hydrolysis using the AH-AC method is ineffective. The resulting RS content is reduced, even lower than only AC [16-19]. On the other hand, hydrolysis of amylopectin by the AC-AH method has been confirmed to significantly increase the RS content of various starches [20-23].

In a previous study, RS3 from corn starch was prepared using the AC-AH method with various acid solutions. It was concluded that hydrolysis with citric acid significantly produced the highest RS contents compared to hydrochloric acid and acetic acid [22]. Several other studies have also reported the effectiveness of citric acids, such as an increase in RS content in green bean starch by 5.0 % after hydrolysis with 0.1 M concentration [20] and an increase in RS content of rice starch by 8.5 % after hydrolysis with 0.15 M concentration [21]. It is likely that RS content will increase as the citric acid concentration increases. However, another study observed that the RS content of corn starch decreased by 1.5 % when the concentration was increased from 0.1 to 0.5 M [23]. Furthermore, the duration of hydrolysis also affects the content of RS produced. It has been observed that there is a significant decrease in RS content when the hydrolysis time exceeds 12 h [23,24].

Each type of starch produces different RS3 properties [25]. Likewise, each preparation method will influence the physicochemical properties and structure of the RS3 results. Up to now, RS3 from tacca tuber starch prepared with AC-AH using citric acid at various concentrations and hydrolysis times has not been reported. Therefore, this research aims to determine the best method for preparing RS3 from tacca tuber starch with AC-AH treatment using citric acid at various concentrations and hydrolysis times and analyze the physicochemical properties and structure of the resulting RS3. This investigation can expand the potential application of tacca tuber starch, a plant species that has been largely neglected and underutilized, as a food source rich in RS. It also seeks

to provide a theoretical basis and technical support for producing RS3.

Materials and methods

Materials

Tacca tubers were obtained from the Garut Coast, West Java, Indonesia. This study used distillate water from Purelizer (Indonesia). The enzymes used were pepsin (Sigma P7000, Sigma-Aldrich, St. Louis, Missouri, USA), α-amylase (Sigma A3306, Sigma-Aldrich, St. Louis, Missouri, USA) and amyloglucosidase (Sigma-Aldrich, St. Louis, Missouri, USA) for measuring RS content. Citric acid and all other chemicals and reagents were of analytical grade from Sigma Chemical Company (Sigma-Aldrich, St. Louis, Missouri, USA).

Starch extraction

Tacca tubers were peeled, washed, crushed and extracted with distilled water in a 1:3 (w/v) ratio until a homogeneous pulp was obtained. This pulp was then filtered using a 60-mesh sieve and squeezed until filtrate 1 was obtained. The remaining pulp was extracted for a second time with distilled water (1:3 w/v) to obtain filtrate 2. Filtrates 1 and 2 were mixed and filtered again using a 200-mesh sieve. Then, it was left for 12 h, and the water was changed every 4 h. Following this, water and sediment were separated. The sediment obtained was wet starch, which was then dried at 50 °C for 24 h. Dried starch was ground to produce a homogeneous starch powder [3].

Preparation of RS3 by AC

The starch suspension was made by mixing 75 mL of distilled water with 25 g of tacca tuber starch in a beaker. The starch suspension was tightly covered using aluminum foil, heated in an autoclave at 121 °C for 30 min, and cooled at 4 °C for 24 h. This procedure was repeated over the course of 2 cycles. It was then continued with the drying process in an oven at 50 °C for 24 h and ground until a homogeneous size was obtained [26]. The RS3 obtained was labeled with the ACs code.

Preparation of RS3 by AC-AH

Tacca tuber starch was initially prepared using the AC method. Then, it was hydrolyzed using citric acid (1:3 w/v) at various concentrations and hydrolysis times (**Table 1**). The process was carried out at room temperature. Each starch that had been hydrolyzed was then neutralized using 0.1 M NaOH and stored at 4 °C for 12 h. The liquid part was disposed of, and the solid part was dried at 50 °C for 24 h. Then, it was ground until a homogeneous size was obtained [20].

Table 1 Hydrolysis conditions and treatment sample codes.

Concentration of citric acid (M)	Hydrolysis time (h)	Code
0.1	4	ACs-AH1
0.1	8	ACs-AH2
0.1	12	ACs-AH3
0.2	4	ACs-AH4
0.2	8	ACs-AH5
0.3	12	ACs-AH6
0.2	4	ACs-AH7
0.3	8	ACs-AH8
0.3	12	ACs-AH9

Determination of proximate composition

The proximate composition of native and RS3 starch, including water, ash, fat and protein content, was determined according to the standard procedures following the AOAC methods [27].

Determination of amylose content

An amount of 50 mg of sample was prepared in a 100 mL volumetric flask, and 1 mL of 96 % ethanol and 9 mL of 1 N NaOH was added. The sample was heated in a water bath at 100 °C for 15 min, then cooled. The volume was adjusted to 100 mL using distilled water. Five mL was pipetted from that volume into a 100 mL measuring flask with 1 mL CH_3COOH 1 N and 2 mL iodine solution, then diluted to 100 mL. Absorbance was measured after 20 min at 625 nm [28]. The amylose content was measured against a standard curve prepared using amylose (Sigma-Aldrich).

Determination of RS content

The enzymatic method was used to determine the RS content of native and RS3 starch. Sample (0.5 g) was mixed with 9 mL buffer trismaleate 0.1 M pH 6.9. Then, it was digested with 1 mL of α-amylase solution (40 mg α-amylase in 1 mL buffer trismaleate) for 30 min at 100 °C using a water bath shaker. The reaction mixture was then cooled to room temperature for 30 min and centrifuged at 3,000 g for 15 min. The residue was collected and washed with distilled water. Then, 6 mL of 2 M KOH was added to each residue and stirred for 30 min at room temperature. The citrate buffer solution was added until the neutral pH was adjusted to 4.4 using 2 M HCl solution. An 80 mL of amyloglucosidase was added, and the mixture was heated in a water bath. It was shaken at 60 °C for 45 min, then cooled to room temperature. Samples were centrifuged (3,000 g, 15 min), and the supernatant was collected. The residue was rewashed with 10 mL of distilled water, and centrifugation was repeated. The washing process was carried out twice. The supernatants obtained were combined and adjusted to a volume of 100 mL using distilled water. The sugar solution was prepared with a concentration of 10 - 60 ppm. Next, 0.5 mL of distilled water, sample and standard were prepared into separate test tubes, and 1 mL of glucose kit reagent (GOD-PAP) was added. It was then stirred until homogeneous and incubated for 30 min at 37 °C using a water bath shaker. Absorbance was read at 500 nm, and sugar concentration was calculated based on a standard curve. The RS content was mg glucose ×0.9 [29].

Determination of swelling power and solubility

The solubility and swelling power of native and RS3 starch were determined using previous methods with slight modifications [30]. A sample of 0.1 g (W) and 10 mL of distilled water were placed in a centrifuge tube and then heated for 30 min at a temperature of 95 °C. After that, the mixture was centrifuged for 30 min at a speed of 3,000 g. The sediment obtained was weighed (Sd), while the supernatant was dried at 105 °C to constant weight and weighed (Su). The solubility and swelling power values are determined based on the following formula:

$$\text{Solubility (\%)} = (Su/W)\times 100\ \% \quad (1)$$

$$\text{Swelling power (g/g)} = (Sd/W)\times(1 - \text{Solubility}) \quad (2)$$

Determination of water holding capacity and oil holding capacity

The water holding capacity (WHC) and oil holding capacity (OHC) of native and RS3 starch were determined using a centrifugal procedure, which was adapted from a previous study [31], with slight modifications. A total of 1 g of sample was placed in a centrifuge tube (known weight), and distilled water (10 mL) or olive oil was added (10 mL). The sample was mixed using a vortex and centrifuged for 10 min at 3,000 g. The supernatant was discarded while the sediment

was weighed. WHC/OHC was measured as grams of water/oil bound by 1 g of dry sample.

Morphology granules observation

Scanning electrons microscopy (SEM) instruments from JEOL (JSM-6510LA, Japan) was used to observe the morphology of native and RS3 starch. The sample was attached to a specimen stub, then coated with carbon tape and treated with gold. The analysis was carried out in a vacuum with an accelerating voltage of 10 kV. Native and RS3 starch morphology was observed at 300× magnification [3].

Determination of crystalline structure

This study used an X-ray diffractometer instrument (Bruker D2 Phaser, Germany) with CuKa radiation nickel filter (λ = 1.542 Å). Samples were initially equilibrated in a saturated relative humidity chamber for 24 h at room temperature, then scanned at a speed of 5 °/min from an area of 5 to 30 °. Amorphous and crystalline diffraction areas were determined using the trial version of OriginPro software (OriginPro 2023, OriginLab Corporation, Northampton, MA, USA). Relative crystallinity (%) was calculated by comparing the crystal area with the total area under the curve [3].

Determination of thermal properties

Thermal properties of native and RS3 starch were determined using the instrument differential scanning calorimetry (DSC) from Shimadzu (DSC-60Plus, Japan), which was equipped with monitoring software (TA-60WS). Samples (4 mg) were prepared in a standard aluminum pan, and 9 μL of distilled water was added. The container was closed tightly and left for 2 h, and the pan was heated at a temperature of 30 - 100 °C with a speed of 10 °C/min in a stream of nitrogen [3]. The thermal properties of starch measured consist of initial temperature (To), peak temperature (Tp), final temperature (Tc), gelatinization temperature range (ΔT) and gelatinization enthalpy (ΔH).

Determination of pasting properties

Pasting properties of native and RS3 starch were evaluated using the Rapid Visco instrument Analyzer (RVA-4500, Perten instruments, Australia) equipped with Thermocline for Windows 3 (TCW3) software. A sample of 3.5 g (14 % moisture base) was put into the container, and 25 g of distilled water was added. The sample mixture was then heated at 50 °C for 1 min, then the temperature was increased to 95 °C with a heating rate of 5.2 °C/min. The sample was left for 5 min at 95 °C. It was then cooled to 50 °C at a speed of 5.2 °C and held at 50 °C for 2 min. The stirring speed for the first 10 s was 960 rpm and maintained at 160 rpm for the remainder of the experiment [3].

Statistical analysis

The study design was a split plot design, where each experiment was conducted in triplicate, and values were presented as the mean standard deviation. The data were analyzed statistically using ANOVA for the difference test. When a significant difference ($p < 0.05$) was identified, further testing was conducted using LSD at a 95 % confidence level with the help of SPSS 17.0 software (SPSS Inc., Chicago, IL, USA).

Results and discussion

Proximate composition

The proximate composition of native and RS3 starch is presented in **Table 2**. The ash content (0.11 - 0.19 %), protein (0.19 - 0.27 %) and lipid (0.19 - 0.29 %) between native and RS3 starch were not significantly different. Thus, the modification does not affect the proximate composition of starch, although its molecular structure may have changed. These results are in line with those observed for RS3 from corn starch (35), as well as acha starch [36]. The low ash, protein, and lipid content shows that native and RS3 starch are very high in purity. A significant difference was observed in the water content of native (10.11 %) and RS3 starch (8.87 - 9.17 %). This difference can be related to changes in

the starch structure after the modification. Amorphous areas that trap much water decrease to form dense crystalline areas. This reason is supported by most studies reporting that modified starch has crystalline regions containing less water [35,37,38].

Amylose content

The amylose content of ACs (37.96 %) increased significantly compared to the native starch (35.33 %). Increased amylose levels in ACs have been amply reported, where the increase in amylose content varied considerably and depended on the type of starch used [11,12,14,18]. It has been reported that hydrothermal processes cause the cleavage of amylopectin chains, leading to the formation of amylose chains [35]. High pressure and temperature during autoclaving partially degrade amylopectin molecules, especially long-chain amylopectin. This process results in more linear amylose chains [39]. Increased amylose content has also been reported in sago starch after AC treatment [40]. In addition, a further increase was observed in ACs-AH1 to ACs-AH9 (41.77 - 51.36 %). This increase was caused by the continuous depolymerization of the amylopectin fraction during the AH treatment. The higher degree of acid hydrolysis, the greater in amylose increases [41]. The AH treatment also causes the formation of intramolecular bonds between amylose and depolymerization of the amylopectin fraction. So that increasing the chain length and the ability to form a complex with iodine, consequently increasing the amylose content [42]. Therefore, this mechanism quite logically explains ACs-AH9 having the highest amylose content.

RS content

The RS content of the native and RS3 is presented in **Table 2**. The RS content of the native starch was 5.33 %, slightly higher than previously reported at 4.25 % [14]. Meanwhile, RS content increased significantly in ACs (18.02 %) and ACs-AH1 to ACs-AH9 (22.94 - 32.40 %). Increased RS content with AC treatment was also reported in arrowroot starch [16], Job's tears starch [25], cowpea starch [39], corn starch [43,44], rice starch [45,46] and black Tartary buckwheat starch [47]. The autoclaving process breaks down starch molecules and makes extensive structural changes. During the cooling process, these molecules combine, resulting in the formation of new structures that are resistant to enzymatic hydrolysis [19]. The formation of RS in ACs is related to the distribution of amylose chains, where more linear amylose chains are more easily retrograded, consequently increasing the formation of RS [40]. ACs consists of crystalline and amorphous regions. Most of the retrograded amylopectin structures in the amorphous region, which has shorter linear chains and easily hydrolyzed by acids [23,48]. During AH, citric acid will make the linear chains of amylopectin to be hydrolyzed into straight chain amylodextrin with a smaller molecular weight [15]. The AH treatment produces small fragments that easily crystallize, so that increasing the presence of RS [48]. In addition, the stability of retrograded starch has been reported to increase with the AH treatment, thereby reducing the enzyme accessibility [43]. However, excessive hydrolysis also reduced RS content, as seen in the ACs-AH8 and ACs-AH9 (**Table 2**). The debranching effect of AH treatment is not as specific as enzymatic hydrolysis, but it is random [23]. Therefore, there is a strong suspicion that excessive AH treatment damages the crystalline regions and increases enzyme accessibility.

Table 2 Proximate composition, amylose and RS contents of native and RS3 starch.

Samples	Moisture (%)	Ash (% db)	Protein (% db)	Lipid (% db)	Amylose (% db)	RS (% db)
Native	10.11 ± 0.07^{b}	0.19 ± 0.01	0.28 ± 0.06	0.28 ± 0.02	35.33 ± 0.10^{a}	5.33 ± 0.17^{a}
ACs	8.87 ± 0.11^{a}	0.16 ± 0.01	0.22 ± 0.02	0.28 ± 0.02	37.96 ± 0.40^{b}	18.02 ± 1.03^{b}
ACs-AH1	8.94 ± 0.04^{a}	0.16 ± 0.02	0.24 ± 0.03	0.25 ± 0.06	41.77 ± 0.89^{c}	22.94 ± 0.80^{c}
ACs-AH2	8.92 ± 0.08^{a}	0.15 ± 0.01	0.23 ± 0.03	0.26 ± 0.05	42.17 ± 0.58^{c}	24.34 ± 0.89^{d}
ACs-AH3	9.07 ± 0.10^{a}	0.14 ± 0.01	0.20 ± 0.03	0.21 ± 0.06	44.38 ± 0.55^{d}	26.48 ± 0.38^{e}
ACs-AH4	9.05 ± 0.15^{a}	0.15 ± 0.01	0.22 ± 0.02	0.23 ± 0.02	44.64 ± 0.33^{d}	26.81 ± 0.40^{e}
ACs-AH5	9.16 ± 0.03^{a}	0.12 ± 0.02	0.23 ± 0.02	0.26 ± 0.07	46.10 ± 0.73^{e}	27.98 ± 0.40^{f}
ACs-AH6	9.15 ± 0.06^{a}	0.13 ± 0.02	0.19 ± 0.05	0.24 ± 0.05	48.29 ± 0.83^{f}	29.20 ± 0.70^{g}
ACs-AH7	9.15 ± 0.09^{a}	0.12 ± 0.03	0.23 ± 0.04	0.19 ± 0.03	49.13 ± 0.58^{f}	32.40 ± 0.38^{h}
ACs-AH8	9.17 ± 0.09^{a}	0.11 ± 0.02	0.23 ± 0.05	0.23 ± 0.02	50.92 ± 0.23^{g}	31.27 ± 0.41^{h}
ACs-AH9	9.13 ± 0.06^{a}	0.12 ± 0.01	0.22 ± 0.04	0.21 ± 0.05	51.36 ± 0.27^{g}	29.75 ± 0.42^{g}

Note: Data represented means ± standard deviations. Values in the same column followed by the same superscript are not significantly different ($p < 0.05$).

Swelling power and solubility

Table 3 shows the swelling power and solubility of native and RS3 starch. The swelling power of native starch was 11.24 %, decreased significantly in ACs (9.65 %). These results align with those observed in AC-modified *Pinellia ternata* starch under the same test conditions [50]. Swelling power is greatly influenced by amylose and amylopectin contained in the starch granules. The stable double helix crystal region of amylopectin will bind water optimally when heated, while amylose will inhibit granule swelling [3,49]. The decrease in swelling power of ACs may be affected by the reduction of hydrophilic groups exposed in the crystalline areas of starch [47]. Apart from that, the swelling power of starch also depends on its capacity to hold water through hydrogen bonds. It is known that the hydrogen bonds between starch molecules are damaged and destroyed during the gelatinization process, and even the molecular chains become weak and disordered [50]. Although the binding interactions of starch molecules increase, this condition causes the loss of double helix formation in starch molecules, thus limiting their swelling power [40,49]. The decrease in swelling power of ACs is also associated with increased crystal perfection and additional interactions between amylose-amylopectin chains [45]. Therefore, the decrease in swelling power was initiated by structural rearrangement and reassociation of starch chains during AC treatment. A further decrease was observed in ACs-AH1 (7.36 %) to ACs-AH9 (4.70 %). The AH treatment destroys the hydrogen bonds between starch polymers. It causes the decay of amorphous areas, resulting in a decrease in swelling strength due to the increase in starch crystalline areas [19,51]. Starch granules with larger crystal areas have stronger bonds and expand less when heated [52]. Therefore, the decrease in the swelling power of RS3 may be caused by the accumulative effects of the gelatinization, autoclaving and acid hydrolysis processes that occurred during sample preparation.

The solubility of the native starch reached 14.59 g/g, which decreased significantly in ACs (5.69 g/g). This decrease may be due to the rearrangement of the starch chain structure after the AC treatment [45]. Apart from that, this can also be associated with the release of amylose and changes in amylose-amylose and amylose-amylopectin interactions, which cause an increase in crystallinity so that the solubility of ACs decreases [53].

Similar observations were also reported in *Pinellia ternata* starch with AC treatment [50]. However, the solubility of RS3 increased from 10.50 to 17.88 g/g after hydrolysis with citric acid. Depolymerization occurs during the AH process, weakening the structure of starch granules and resulting in increased solubility. The AH treatment damages the microcrystalline structure of starch and makes the intermolecular network structure relatively loose due to the leaching of amylose and the degradation of the amylopectin component [53,54].

Table 3 Functional properties of native and RS3 starch.

Samples	Swelling Power (%)	Solubility (g/g)	WHC (g/g)	OHC (g/g)
Native	11.24 ± 0.31^{g}	14.59 ± 0.60^{d}	0.78 ± 0.02^{a}	0.67 ± 0.01^{b}
ACs	9.65 ± 0.33^{f}	5.69 ± 0.48^{a}	3.12 ± 0.03^{g}	0.53 ± 0.00^{a}
ACs-AH1	7.36 ± 0.19^{e}	10.50 ± 0.22^{b}	2.95 ± 0.01^{f}	0.56 ± 0.00^{a}
ACs-AH2	7.17 ± 0.16^{e}	10.76 ± 0.58^{b}	2.94 ± 0.02^{ef}	0.59 ± 0.01^{a}
ACs-AH3	6.56 ± 0.15^{d}	11.94 ± 0.65^{c}	2.91 ± 0.01^{e}	0.59 ± 0.00^{a}
ACs-AH4	5.62 ± 0.34^{c}	14.44 ± 0.61^{d}	2.86 ± 0.01^{d}	0.57 ± 0.01^{a}
ACs-AH5	5.05 ± 0.15^{b}	16.81 ± 0.11^{e}	2.84 ± 0.01^{cd}	0.59 ± 0.00^{a}
ACs-AH6	4.89 ± 0.04^{ab}	17.06 ± 0.76^{ef}	2.82 ± 0.01^{bc}	0.60 ± 0.00^{a}
ACs-AH7	4.87 ± 0.09^{ab}	17.80 ± 0.19^{f}	2.82 ± 0.03^{bc}	0.59 ± 0.01^{a}
ACs-AH8	4.86 ± 0.06^{ab}	17.86 ± 0.01^{f}	2.80 ± 0.01^{b}	0.60 ± 0.00^{a}
ACs-AH9	4.70 ± 0.29^{a}	17.88 ± 0.12^{f}	2.81 ± 0.02^{b}	0.61 ± 0.00^{a}

Note: Data represented means ± standard deviations. Values in the same column followed by the same superscript are not significantly different ($p < 0.05$).

WHC and OHC

The AC treatment significantly increased the WHC of ACs (3.12 g/g) compared to native starch (0.78 g/g). These results are consistent with those reported for cowpea and taro starch modified by AC treatment [39,55]. WHC is related to hydrogen bonds between starch chains. Native starch has more hydrogen bonds and covalent bonds between chains, so there are fewer sites available for water binding, and therefore the WHC of native starch is lower [56]. On the other hand, the autoclaving process causes partial degradation of amylopectin chains and the breakdown of hydrogen bonds, resulting in the formation of lower molecular weight starch granules with higher affinity to water molecules, so the WHC of ACs increase [39,50]. AC-AH treatment resulted in a WHC of 2.80 to 2.95 g/g, decreasing significantly compared to ACs. The decrease in WHC is affected by the reduction of amorphous areas, which are responsible for binding water in starch granules [19]. In contrast to WHC, the OHC of the native starch (0.67 g/g) was higher than that of ACs (0.53 g/g) and ACs-AH1 to ACs-AH9 (0.56 - 0.61 g/g). On the other hand, OHC between RS3 did not show significant differences. OHC is associated with the physical trapping of oil through capillary attraction, which is related to the presence of pores [37]. The increase in the crystalline area due to the modification can be attributed to the decrease in the OHC of RS3. In addition, the modification process rearranges the linear amylose chains in the increasingly dense regions of starch crystals and forms a double helix, resulting in lower porosity and consequently limiting oil absorption [57]. These results are consistent with those reported for

modified arrowroot starch [16] and modified acha starch [51].

Color profile

The color profile of the native starch and RS3 are presented in **Table 4**. All color parameters (L*, a*, b* and WI values) are influenced by the AC and AC-AH treatment. The AC treatment causes a significant decrease in the brightness and whiteness index values of the ACs. On the other hand, the AH treatment increased the brightness value and whiteness index of starch. This increase is linear to the level of concentration and hydrolysis time. However, the brightness and whiteness index values of ACs were lower than those of the native starch. It has been widely reported that the combination of heat and pressure during the autoclave process has a negative influence on the brightness and whiteness index values of the modified starch [35,45]. The decrease in the brightness and whiteness index values of ACs is attributed to the non-enzymatic browning effect resulting from the Maillard reaction between reducing sugars from heated starch and amino groups in proteins during treatment [39,58]. At the same time, the hydrolysis effect of the acid solution causes color degradation in starch [18]. Thus, the color pigments produced during the Maillard reaction in the AC process are degraded during the AH process. The phenomenon of increasing starch brightness and whiteness index due to acid hydrolysis has also been reported for rice berry rice starch [19], arrowroot starch [16], acha starch and iburu starch [51]. All starch samples had low a* (−0.22 to 0.61) and b* (1.94 to 3.56) values, so the differences were not visually visible. The color change of ACs was the greatest compared to the native starch, with an ΔE* value of 7.73. The ΔE* value of ACs-AH1 (6.33) to ACs-AH9 (2.22) decreased significantly. This means AC-AH treatment produces an RS3 color profile close to the native starch color.

Table 4 Color profile of native and RS3 starch.

Samples	L*	a*	b*	WI	ΔE*
Native	93.53 ± 0.27^{h}	-0.22 ± 0.01^{a}	1.94 ± 0.03^{a}	93.24 ± 0.26^{i}	-
ACs	86.03 ± 0.83^{a}	0.61 ± 0.30^{b}	3.56 ± 0.42^{e}	85.56 ± 0.81^{a}	7.73 ± 0.83^{h}
ACs-AH1	87.32 ± 0.09^{b}	0.50 ± 0.21^{b}	2.90 ± 0.06^{d}	86.98 ± 0.09^{b}	6.33 ± 0.07^{g}
ACs-AH2	88.28 ± 0.25^{c}	0.42 ± 0.13^{b}	2.58 ± 0.07^{c}	87.99 ± 0.23^{c}	5.33 ± 0.24^{f}
ACs-AH3	88.96 ± 0.16^{d}	0.31 ± 0.10^{b}	2.29 ± 0.09^{b}	88.72 ± 0.14^{d}	4.61 ± 0.15^{e}
ACs-AH4	89.17 ± 0.20^{d}	0.30 ± 0.17^{b}	2.29 ± 0.13^{b}	88.93 ± 0.19^{e}	4.41 ± 0.15^{e}
ACs-AH5	89.30 ± 0.16^{d}	0.30 ± 0.08^{b}	2.31 ± 0.03^{b}	89.05 ± 0.15^{e}	4.28 ± 0.15^{e}
ACs-AH6	89.85 ± 0.13^{e}	0.30 ± 0.10^{b}	2.16 ± 0.06^{ab}	89.62 ± 0.13^{f}	3.72 ± 0.14^{d}
ACs-AH7	90.34 ± 0.34^{f}	0.18 ± 0.16^{b}	2.12 ± 0.19^{ab}	90.11 ± 0.35^{g}	3.22 ± 0.35^{c}
ACs-AH8	90.88 ± 0.15^{g}	0.16 ± 0.05^{b}	2.09 ± 0.14^{a}	90.65 ± 0.17^{g}	2.68 ± 0.15^{b}
ACs-AH9	91.36 ± 0.45^{g}	0.22 ± 0.06^{b}	1.99 ± 0.03^{a}	91.13 ± 0.44^{h}	2.22 ± 0.45^{a}

Note: Data represented means ± standard deviations. Values in the same column followed by the same superscript are not significantly different ($p < 0.05$).

Granule morphology

The morphology of the native and RS3 granules is presented in **Figure 1**. The native starch granules of tacca tubers are polygonal, elliptical and oval with a smooth surface, according to previous reports [3]. All RS3 granules undergo deformation. AC treatment changes the shape and surface of ACs granules into a more compact structure, irregular, rough surface, many-

layered lines (arrow 1), a non-homogeneous shape and many cracks. Some starch granules aggregated, indicating that AC treatment can form a cohesive mass of starch granules. The changes in ACs granule morphology are caused by the limited water content and thermal forces applied to the starch during the treatment. Water absorption during heating increases the mobility of starch molecules, which causes the molecules to expand and promotes morphological changes in the granules. Apart from that, it is also caused by the partial gelatinization melting process on the surface of the starch granules, which is helped by adding water and heat [19,35,46]. The rough surface and numerous layered lines on the surface of ACs are caused by the leaching of amylose from starch, loss of amylopectin crystalline regions during heating, and reassociation of starch chains in granules [39,50]. The same thing happened to all RS3 from AC-AH treatment. In addition, the surface of ACs-AH1 to ACs-AH9 appears rougher, as if it has been eroded (2 arrows). The increasingly rough surface results from the erosion process due to AH treatment. Acid usually acts on the internal structure of starch granules; the presence of cracks provides access for acid to penetrate the granule structure [59]. In addition, these acids prefer attacking the granule surface and consequently degrading starch molecules, causing fragmentation [60]. The fragments formed are usually smaller and crystallize easily. The fragments formed increase the proportion of crystalline parts, this increase in crystalline structure is mainly responsible for the increased resistance to enzymatic hydrolysis [48].

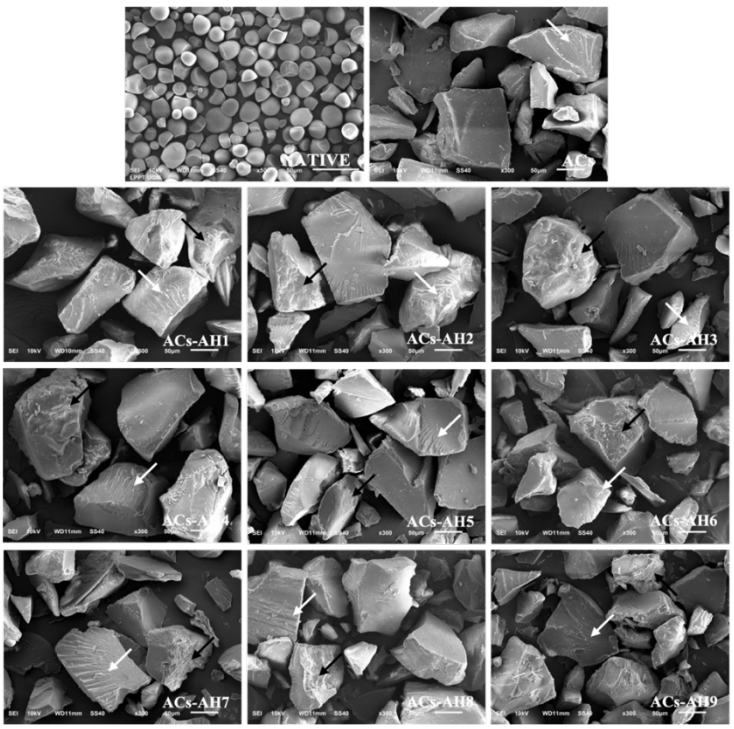

Figure 1 Scanning electron micrograph of native and RS3 starch.

Crystalline structures

The crystallinity of the native and RS3 starch is presented in **Figure 2**. The X-RD pattern of native starch has strong peaks at 15, 17 and 23 ° 2θ, then 1 shoulder peak at 18° 2θ (**Figure 2(A)**) which indicates a CA-type crystal structure. The same pattern was also found in arrowroot, cassava and sweet potato starch [4,61]. The XRD pattern of RS3 undergoes significant changes compared to the native starch. The crystal structure of RS3 was transformed into a combination of

types B (single peaks: 15, 17 and 22 ° 2θ) and V (weak peak around 20 ° 2θ). These findings are consistent with those reported previously [25,43,62]. The change in crystalline structure from type CA to type B is related to the retrogradation process of starch gel at low temperatures. At the same time, the V-type starch crystal structure is formed under the influence of high temperature during the autoclaving process, which causes an increase in the stability of the single helical chain [39]. Besides that, typical helical crystallites of amylose can also form a V-type crystal structure in certain types of starch, which is stabilized by adding lipophilic compounds [63]. During the AC treatment, the fluidity of starch increases, causing structural changes in the crystalline regions, causing an increase in crystallinity.

Although it did not change the XRD pattern, AC-AH treatment showed a tendency to increase relative crystallinity, consistent with previously reported results [59]. The autoclaving treatment causes the amylose chains to be released, while the AH treatment causes the branched amylopectin chains to break. This process allows aggregation at low temperatures, where the double helix structure can form higher and organize into stronger crystalline regions [60]. When acid molecules penetrate the crystalline area, the surface layer of the crystalline area will be damaged, and an erosion phenomenon occurs. This is proven by the morphological structure of ACs-AH1 to ACs-AH9 (**Figure 1**) showing aggregated and fragmented parts. The crystallinity results show that the short chains obtained from AH treatment can easily form a double helix structure with stronger crystalline areas. However, in conditions where AH is too high, excessive hydrolysis occurs, causing a weakening of the double helix structure in the crystalline area. Although the crystal structure does not change, the relative crystallinity decreases. A decrease in starch crystallinity under conditions of too high AH was also observed in sweet potato starch and potato starch [41,64]. The crystallinity decrease may be caused by an increase in the proportion of disordered short chains [59]. Starch crystallinity is closely related to crystal size, the amount of crystallinity, the orientation of the double helix, and the degree of interaction between the double helices [29]. The crystallinity of RS3 has the same pattern as the RS content presented in **Table 2**.

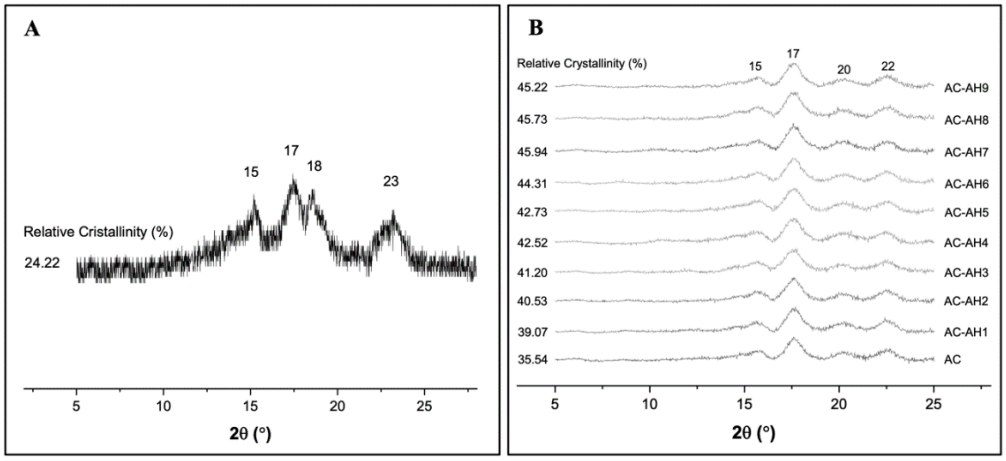

Figure 2 X-ray diffraction pattern of (A) native and (B) RS3 starch.

Thermal properties

The thermal properties of starch measured consist of initial temperature (To), peak temperature (Tp), final temperature (Tc), gelatinization temperature range (ΔT) and gelatinization enthalpy (ΔH). **Table 5** summarizes the thermal properties of native and RS3 starch. The

gelatinization temperature of native starch ranges from 58.57 to 70.96 °C (Tc), where the Tp of starch is around 60.56 °C, ΔT is 12.39 °C and ΔH is 3.96 J/g. The AC process significantly increased To (133.18 °C), Tp (135.6 °C), Tc (142.00 °C) and AH (5.68 Jg) of ACs, while ΔT (8.82 °C) decreased significantly. A similar increase was also observed in the thermal profile of ACs-AH1 to ACs-AH9, with values of To (135.36 - 143.04 °C), Tp (135.76 - 146.14 °C), Tc (142.00 - 153.86 °C), ΔT (9.09 - 10.82 °C) and ΔH (6.11 - 15.25 J/g) increased significantly compared to ACs. Increasing the gelatinization temperature shows that AC treatment produces ACs that is more stable and more resistant to the gelatinization process. The increase in To, Tp and Tc of ACs indicates a stronger interaction between amylose and the outer branches of amylopectin, thus requiring a higher temperature to disrupt the crystalline regions [39]. An increase in To is associated with forming long-chain double-helix amylose crystallites. In contrast, an increase in Tp is associated with an increase in the regularity and stability of the double helix structure through hydrogen bonds and other intermolecular forces [65]. The decrease in ΔT of ACs indicates that the AC treatment produces a more homogeneous and perfect crystalline structure, which is responsible for the better resistance of RS3 [25,45]. On the other hand, ΔT from ACs-AH1 to ACs-AH9 tends to increase, so it can be assumed that AC-AH treatment produces more heterogeneous crystals.

Table 5 Thermal properties of native and RS3 starch.

Samples	T_o (°C)	T_p (°C)	T_c (°C)	ΔT (°C)	ΔH (J/g)
Native	58.57 ± 0.08^{a}	60.56 ± 0.28^{a}	70.96 ± 0.16^{a}	12.39 ± 0.07^{d}	3.96 ± 0.01^{a}
ACs	133.18 ± 0.28^{b}	135.76 ± 0.35^{b}	142.00 ± 0.27^{b}	8.82 ± 0.01^{a}	5.68 ± 0.20^{b}
ACs-AH1	135.36 ± 0.40^{c}	138.25 ± 0.26^{c}	144.45 ± 0.15^{c}	9.09 ± 0.27^{a}	6.11 ± 0.36^{c}
ACs-AH2	137.39 ± 0.20^{d}	139.93 ± 0.24^{d}	147.26 ± 0.27^{d}	9.86 ± 0.40^{b}	7.21 ± 0.11^{d}
ACs-AH3	138.61 ± 0.26^{e}	141.29 ± 0.15^{e}	148.49 ± 0.44^{e}	9.87 ± 0.43^{b}	7.55 ± 0.16^{d}
ACs-AH4	139.50 ± 0.43^{f}	142.20 ± 0.47^{f}	149.44 ± 0.34^{f}	9.94 ± 0.70^{b}	7.68 ± 0.28^{d}
ACs-AH5	140.11 ± 0.14^{g}	142.72 ± 0.20^{f}	150.19 ± 0.10^{g}	10.07 ± 0.24^{b}	9.31 ± 0.06^{e}
ACs-AH6	140.89 ± 0.12^{h}	143.81 ± 0.31^{g}	151.00 ± 0.09^{h}	10.11 ± 0.20^{b}	10.18 ± 0.10^{f}
ACs-AH7	143.04 ± 0.07^{k}	146.14 ± 0.11^{h}	153.86 ± 0.09^{j}	10.82 ± 0.15^{c}	15.25 ± 0.22^{h}
ACs-AH8	142.12 ± 0.10^{j}	144.31 ± 0.37^{g}	152.55 ± 0.13^{i}	10.43 ± 0.06^{c}	13.61 ± 0.08^{f}
ACs-AH9	141.04 ± 0.13^{i}	143.96 ± 0.40^{g}	151.17 ± 0.09^{h}	10.13 ± 0.05^{b}	10.37 ± 0.07^{d}

Note: Data represented means ± standard deviations. Values in the same column followed by the same superscript are not significantly different ($p < 0.05$).

The ΔH value represents the energy required to break the double helix structure during starch gelatinization. Native starch has the lowest ΔH, associated with a weak starch matrix or network that requires less energy to disrupt its molecular organization. The increase in ΔH value of ACs confirms that during the retrogradation stage there is an increase in interaction between amylose and the outer branches of amylopectin which results in efficient packing due to the formation of a double helix [45]. The amorphous areas remaining in the starch granules will form fragments that easily crystallize after hydrolysis, as a result increasing the energy required for gelatinization [48]. ΔH itself is influenced by several things, such as the degree of order, the degree of the double helix and relative crystallinity [35]. The highest ΔH was observed

in ACs-AH7, which had the highest relative crystallinity (**Figure 2**). Thus, the decrease in ΔH in ACs-AH8 and ACs-AH9 is closely related to the decrease in relative crystallinity. In addition, the weakening of the internal network due to the AH treatment can also lead to the formation of irregular short chains in starch granules [51,59]. In general, the heat resistance of RS3 is better than native starch's. This is related to the crystalline structure of RS3 having a high density and stable crystal regions [66]. Starch with these characteristics is proposed to be more resistant to processing [67].

Pasting properties

In general, the modification caused significant changes in the properties of the starch paste (**Table 6**). Pasting temperature (PT) of ACs (56.53 °C) was lower than native starch (72.61). The PT value increased significantly from ACs-AH1 (57.82 °C) to ACs-AH9 (60.08 °C). The low PT in ACs indicates that the RS3 is more difficult to swell [39], this is affected by damage to the starch granules during autoclaving at high temperatures [68]. A reduction in PT with the AC treatment was also reported in ACs from taro starch [55], elephant foot yam starch [68], arrowroot starch [16], Job's tears starch [25] and cowpea starch [39]. However, some studies reported the opposite, such as in ACs from rice starch and corn starch which was associated with an increase in the relative crystallinity of the starch [44,45]. PT of ACs is not only influenced by relative crystallinity but also by other factors such as amylose-amylose, amylose-amylopectin interactions, amylopectin-amylopectin interactions and the formation of intermolecular hydrogen bonds [55]. The AC treatment also causes a decrease in peak viscosity (PV), through viscosity (TV), breakdown viscosity (BV), final viscosity (FV) and setback viscosity (SV) of ACs, which is effect of exposure to very high heat and pressure during autoclaving. As a result, the starch undergoes gelatinization, and the granule structure is disturbed, causing the paste profile to decrease [69]. The decrease in viscosity value is closely related to the level of damage to the starch structure by the AC treatment [16].

Table 6 Pasting properties of native and RS3 starch.

Samples	PT (°C)	PV (cP)	TV (cP)	BV (cP)	FV (cP)	SV (cP)
Native	72.61 ± 0.11^{j}	$4,822.50 \pm 88.39^{i}$	$1,458.00 \pm 32.53^{i}$	$3,364.50 \pm 55.86^{g}$	$2,856.00 \pm 53.74^{k}$	$1,398.00 \pm 21.21^{i}$
ACs	56.53 ± 0.13^{a}	$2,743.33 \pm 48.56^{h}$	$1,450.33 \pm 27.93^{i}$	$1,293.00 \pm 67.62^{f}$	$2,658.33 \pm 49.52^{j}$	$1,208.00 \pm 75.99^{h}$
ACs-AH1	57.82 ± 0.08^{b}	$2,486.67 \pm 20.01^{g}$	$1,476.00 \pm 10.15^{h}$	$1,010.67 \pm 10.26^{e}$	$2,505.33 \pm 10.02^{i}$	$1,029.33 \pm 20.03^{g}$
ACs-AH2	58.28 ± 0.16^{c}	$1,950.67 \pm 10.41^{f}$	$1,421.67 \pm 10.12^{g}$	529.00 ± 19.08^{d}	$2,121.00 \pm 10.54^{h}$	699.33 ± 20.26^{f}
ACs-AH3	58.62 ± 0.10^{d}	$1,816.67 \pm 10.12^{e}$	$1,377.33 \pm 10.02^{f}$	439.33 ± 14.98^{c}	$1,962.67 \pm 10.02^{g}$	585.33 ± 17.90^{e}
ACs-AH4	58.88 ± 0.06^{e}	$1,406.00 \pm 10.15^{d}$	970.67 ± 20.03^{e}	435.33 ± 10.02^{c}	$1,220.67 \pm 10.97^{f}$	250.00 ± 10.44^{d}
ACs-AH5	59.03 ± 0.03^{ef}	$1,138.67 \pm 10.07^{c}$	779.33 ± 18.15^{d}	359.33 ± 28.02^{b}	973.67 ± 10.02^{e}	194.33 ± 10.12^{c}
ACs-AH6	59.17 ± 0.08^{f}	964.67 ± 10.02^{b}	745.00 ± 10.54^{c}	219.67 ± 20.50^{a}	931.00 ± 10.58^{d}	186.00 ± 20.95^{bc}
ACs-AH7	59.57 ± 0.08^{g}	$1,145.67 \pm 12.01^{c}$	735.00 ± 10.00^{c}	410.67 ± 11.59^{c}	898.67 ± 10.69^{c}	163.67 ± 12.01^{abc}
ACs-AH8	59.80 ± 0.05^{h}	820.00 ± 19.00^{a}	613.00 ± 10.15^{b}	207.00 ± 10.44^{a}	771.67 ± 10.21^{b}	158.67 ± 19.60^{ab}
ACs-AH9	60.08 ± 0.03^{i}	806.67 ± 10.41^{a}	579.33 ± 20.13^{a}	227.33 ± 10.03^{a}	723.00 ± 11.27^{a}	143.67 ± 10.41^{a}

Note: Data represented means ± standard deviations. Values in the same column followed by the same superscript are not significantly different ($p < 0.05$). PT.

The AH process clearly reduces the viscosity of RS3 due to the disruption of amorphous areas. This phenomenon becomes more visible as the concentration and hydrolysis time increase. These results are consistent with previous findings [54,70]. The AH treatment causes partial debranching of the amylopectin molecules, and the internal cohesion in the starch matrix weakens, resulting in erosion of the granules [51]. During heating, the breakdown of starch molecules in the amorphous region limits water absorption so that the starch granules do not reach maximum swelling capacity [54]. If the acid conditions are too high, the

viscosity of the paste weakens and can even be ignored [71]. The decrease in viscosity due to the AH treatment indicates the easy polymerization of starch with this treatment [51]. Changes in the structure of amylopectin chains due to acid treatment may be associated with a decrease in FV. ACs-AH9 had the lowest SV of all modified starches, which may be due to the formation of short-chain amylose during the AH process and the degradation of longer branched-chain amylopectin. Interestingly, RS3 with low SV shows good paste stability during cooling [70]. Pastes with these properties produce more fluid gels so that they can be applied to various types of food products. In general, the higher RS content, the lower viscosity and water absorption capacity. The result in this study indicates that RS3 is resistant to granule swelling. The AH process can affect the arrangement of starch granules, but the RS produced does not melt during the heating process [64]. This proves that apart from being beneficial for health, the RS3 produced can also be applied to food products that require high gel stability.

Conclusions

AC and AC-AH treatments generally affected tacca tuber starch's physicochemical properties and RS3 structure. The addition of citric acid concentration and hydrolysis time in the AC-AH treatment did not affect the proximate composition (except for moisture content). However, there has been an increase in amylose content, RS content, solubility, OHC, color profile, relative crystallinity, thermal profile and pasting temperature. This increase was also accompanied by changes in the crystalline structure and morphology of RS3, as well as a decrease in swelling power, WHC and paste profile. ACs-AH7 is recommended because it contains the highest levels of RS and few impurities. The amylose content of ACs-AH7 reaches 49.13 %, so it has limited swelling power with low of solubility, WHC and OHC. The brightness value and whiteness index of ACs-AH7 are very high, close to native starch. ACs-AH7 has an irregular morphology with a very rough and lumpy surface. The crystal structure of ACs-AH7 is a mixture of types B and V, with a relative crystallinity of 45.94 %, so it has a good thermal and a paste profile with high gel stability, so it does not thicken during cooling. RS3 tuber starch has the potential to be applied to food products that require good paste stability, such as porridge and ice cream.

Acknowledgements

The authors gratefully acknowledge to Ministry of Education, Culture, Research and Technology, the Republic of Indonesia for financial support through the program of Doctoral Dissertation Grant with contract No. 3123/UN1/DITLIT/Dit-Lit/PT.01.03/2023

References

[1] TK Lim. *Tacca leontopetaloides. In*: TK Lim (Ed.). Edible medicinal and non-medicinal plants. Springer, Netherlands, 2016, p. 301-307.

[2] D Yonata, B Pranata and Nurhidajah. Potential of neglected and underutilized tacca tuber (*Tacca leontopetaloides*) for sustainable food system in Indonesia. *Journal of Global Innovations in Agricultural Sciences* 2024; **12(3)**, 770-778.

[3] D Yonata, P Triwitono, LA Lestari and Y Pranoto. Physicochemical, structure and functional characteristics of *Tacca leontopetaloides* starches grown in Indonesia. *Biodiversitas Journal of Biological Diversity* 2023; **24(11)**, 6396-6406.

[4] L Zhang, L Zhao, X Bian, K Guo, L Zhou and C Wei. Characterization and comparative study of starches from seven purple sweet potatoes. *Food Hydrocolloids* 2018; **80**, 168-176.

[5] Q Chang, B Zheng, Y Zhang and H Zeng. A comprehensive review of the factors influencing the formation of retrograded starch. *International Journal of Biological Macromolecules* 2021; **186**, 163-173.

[6] Q Liu, J Shi, Z Jin and A Jiao. Development and characterization of resistant starch produced by an extrusion - debranching strategy with a high starch concentration. *Food Hydrocolloids* 2023; **136**, 108276.

[7] M Meenu and B Xu. A critical review on anti-diabetic and anti-obesity effects of dietary resistant starch. *Critical Reviews in Food Science and Nutrition* 2019; **59(18)**, 3019-3031.

[8] Y Pranoto. *Starch and its derivatives as potential source of prebiotics*. *In*: PS Panesar and AK Anal (Eds.). Probiotics, prebiotics and synbiotics: Technological advancements toward safety and industrial applications. Wiley, England, 2022. p. 378-406.

[9] Z Ma, X Hu and JI Boye. Research advances on the formation mechanism of resistant starch type III: A review. *Critical Reviews in Food Science and Nutrition* 2020; **60(2)**, 276-297.

[10] Y Zhang, W Liu, C Liu, S Luo, T Li, Y Liu, D Wu and Y Zuo. Retrogradation behaviour of high-amylose rice starch prepared by improved extrusion cooking technology. *Food Chemistry* 2014; **158**, 255-261.

[11] VF Abioye, IA Adeyemi, BA Akinwande, P Kulakow and B Maziya-Dixon. Effect of autoclaving on the formation of resistant starch from two Nigeria Cassava (*Manihot esculenta*) varieties. *Food Research* 2018; **2(5)**, 468-473.

[12] G Giuberti, A Marti, A Gallo, S Grassi and G Spigno. Resistant starch from isolated white sorghum starch: Functional and physicochemical properties and resistant starch retention after cooking. A comparative study. *Starch* 2019; **71(7-8)**, 1800194.

[13] F Zheng, Q Xu, S Zeng, Z Zhao, Y Xing, J Chen and P Zhang. Multi-scale structural characteristics of black Tartary buckwheat resistant starch by autoclaving combined with debranching modification. *International Journal of Biological Macromolecules* 2023; **249**, 126102.

[14] ERN Herawati, D Ariani, R Nurhayati, M Miftakhussolikhah, H Na'imah and Y Marsono. Effect of autoclaving-cooling treatments on chemical characteristic and structure of Tacca (*Tacca leontopetaloides*) starch. *In*: Proceedings of the 5th International Conference on Food, Agriculture and Natural Resources, Paris, France. 2020, p. 169-172.

[15] S Ozturk, H Koksel and PKW Ng. Production of resistant starch from acid-modified amylotype starches with enhanced functional properties. *Journal of Food Engineering* 2011; **103(2)**, 156-164.

[16] RM Astuti, Widaningrum, N Asiah, A Setyowati and R Fitriawati. Effect of physical modification on granule morphology, pasting behavior, and functional properties of arrowroot (*Marantha arundinacea* L) starch. *Food Hydrocolloids* 2018; **81**, 23-30.

[17] TAA Nasrin and AK Anal. Resistant starch III from culled banana and its functional properties in fish oil emulsion. *Food Hydrocolloids* 2014; **35**, 403-409.

[18] S Raungrusmee and AK Anal. Effects of lintnerization, autoclaving, and freeze-thaw treatments on resistant starch formation and functional properties of Pathumthani 80 rice starch. *Foods* 2019; **8(11)**, 558.

[19] S Raungrusmee, S Koirala and AK Anal. Effect of physicochemical modification on granule morphology, pasting behavior, and functional properties of Riceberry rice (*Oryza Sativa* L.) starch. *Food Chemistry Advances* 2022; **1**, 100116.

[20] P Triwitono, Y Marsono, A Murdiati and DW Marseno. The effect of two cycles autoclaving and citric acid hydrolysis combination to chemical and physical characteristics of mung beans (*Vigna*

radiata L.) starch RS-3. *Agritech* 2018; **37(3)**, 312-318.

[21] F Fan, X Huxi, L Qinlu, Z Qian, W Suyan, L Feijun and Y Ya. Ultrasound-damp heat method combined with acid hydrolysis in preparation of rice resistant starch and its physico-chemical properties. *Journal of the Chinese Cereals and Oils Association* 2018; **33(7)**, 43-50.

[22] XH Zhao and Y Lin. Resistant starch prepared from high-amylose maize starch with citric acid hydrolysis and its simulated fermentation *in vitro*. *European Food Research and Technology* 2009; **228(6)**, 1015-1021.

[23] XH Zhao and Y Lin. The impact of coupled acid or pullulanase debranching on the formation of resistant starch from maize starch with autoclaving-cooling cycles. *European Food Research and Technology* 2009; **230**, 179-184.

[24] WSW Pratiwi, AK Anal and SR Putra. Production by lintnerization-autoclaving and physicochemical characterization of resistant starch III from sago palm (*Metroxylon sagu* rottb). *Indonesian Journal of Chemistry* 2015; **15(3)**, 295-304.

[25] Q Yang, L Liu, X Li, J Li, W Zhang, M Shi and B Feng. Physicochemical characteristics of resistant starch prepared from Job's tears starch using autoclaving-cooling treatment. *CyTA - Journal of Food* 2021; **19(1)**, 316-325.

[26] R Nurhayati, AN Suryadi, D Ariani, ERN Herawati, Miftakhussolikhah and Y Marsono. Resistant starch in native Tacca (*Tacca leontopetaloides*) starch and its various modified starches. *International Food Research Journal* 2022; **29(3)**, 667-675.

[27] AOAC International. *Official methods of analysis*. AOAC International, Washington DC, 1995.

[28] MA Zailani, H Kamilah, A Husaini, AZRA Seruji and SR Sarbini. Functional and digestibility properties of sago (*Metroxylon sagu*) starch modified by microwave heat treatment. *Food Hydrocolloids* 2022; **122**, 107042.

[29] Y Zhou, S Meng, D Chen, X Zhu and H Yuan. Structure characterization and hypoglycemic effects of dual modified resistant starch from indica rice starch. *Carbohydrate Polymers* 2014; **103**, 81-86.

[30] M Wang, G Liu, J Li, W Wang, A Hu and J Zheng. Structural and physicochemical properties of resistant starch under combined treatments of ultrasound, microwave, and enzyme. *International Journal of Biological Macromolecules* 2023; **232**, 123331.

[31] YC Koh and HJ Liao. Preparation and physicochemical characterization of debranched rice starch nanoparticles from mono- and dual-modification by hydrothermal treatments. *Food Bioscience* 2023; **55**, 103004.

[32] JB Hutchings. *Food colour and appearance*. Springer, Boston, 1999.

[33] K Zhu, PJ Kanu, IP Claver, K Zhu, H Qian and H Zhou. A method for evaluating Hunter whiteness of mixed powders. *Advanced Powder Technology* 2009; **20(2)**, 123-126.

[34] WS Mokrzycki and M Tatol. Color difference delta E - A survey. *Machine Graphics and Vision* 2011; **20(4)**, 383-411.

[35] H Marta, Y Cahyana, S Bintang, GP Soeherman and M Djali. Physicochemical and pasting properties of corn starch as affected by hydrothermal modification by various methods. *International Journal of Food Properties* 2022; **25(1)**, 792-812.

[36] I Isah, AA Oshodi and VN Atasie. Physicochemical properties of cross linked acha (*Digitaria exilis*) starch with citric acid. *Chemistry International* 2017; **3(2)**, 150-157.

[37] MA Zailani, H Kamilah, A Husaini and SR Sarbini. Physicochemical properties of microwave

heated sago (*Metroxylon sagu*) starch. *CyTA - Journal of Food* 2021; **19(1)**, 596-605.

[38] W Sangwongchai, N Sa-ingthong, S Phothiset, C Saenubon and M Thitisaksakul. Resistant starch formation and changes in physicochemical properties of waxy and non-waxy rice starches by autoclaving-cooling treatment. *International Journal of Food Properties* 2024; **27(1)**, 532-548.

[39] N Ratnaningsih, Suparmo, E Harmayani and Y Marsono. Physicochemical properties, *in vitro* starch digestibility, and estimated glycemic index of resistant starch from cowpea (*Vigna unguiculata*) starch by autoclaving-cooling cycles. *International Journal of Biological Macromolecules* 2020; **142**, 191-200.

[40] RSA Rashid, AMD Mohamed, SN Achudan and P Mittis. Physicochemical properties of resistant starch type III from sago starch at different palm stages. *Materials Today: Proceedings* 2020; **31**, 150-154.

[41] AS Babu, R Parimalavalli, K Jagannadham and JS Rao. Chemical and structural properties of sweet potato starch treated with organic and inorganic acid. *Journal of Food Science and Technology* 2015; **52(9)**, 5745-5753.

[42] AS Babu, R Parimalavalli and SG Rudra. Effect of citric acid concentration and hydrolysis time on physicochemical properties of sweet potato starches. *International Journal of Biological Macromolecules* 2015; **80**, 557-565.

[43] NH Kim, JH Kim, S Lee, H Lee, JW Yoon, R Wang and SH Yoo. Combined effect of autoclaving-cooling and cross-linking treatments of normal corn starch on the resistant starch formation and physicochemical properties. *Starch* 2010; **62(7)**, 358-363.

[44] AN Dundar and D Gocmen. Effects of autoclaving temperature and storing time on resistant starch formation and its functional and physicochemical properties. *Carbohydrate Polymers* 2013; **97(2)**, 764-771.

[45] BA Ashwar, A Gani, IA Wani, A Shah, FA Masoodi and DC Saxena. Production of resistant starch from rice by dual autoclaving-retrogradation treatment: *In vitro* digestibility, thermal and structural characterization. *Food Hydrocolloids* 2016; **56**, 108-117.

[46] H Li, Y Gui, J Li, Y Zhu, B Cui and L Guo. Modification of rice starch using a combination of autoclaving and triple enzyme treatment: Structural, physicochemical and digestibility properties. *International Journal of Biological Macromolecules* 2020; **144**, 500-508.

[47] Q Xu, F Zheng, P Yang, P Tu, Y Xing, P Zhang, H Liu, X Liu and X Bi. Effect of autoclave–cooling cycles combined pullulanase on the physicochemical and structural properties of resistant starch from black Tartary buckwheat. *Journal of Food Science* 2023; **88(1)**, 315-327.

[48] H Kim, KH Lee, JY Kim, WJ Lim and ST Lim. Characterization of nanoparticles prepared by acid hydrolysis of various starches. *Starch* 2012; **64(5)**, 367-373.

[49] Y Pranoto, Rahmayuni, Haryadi and SK Rakshit. Physicochemical properties of heat moisture treated sweet potato starches of selected Indonesian varieties. *International Food Research Journal* 2014; **21(5)**, 2031-2038.

[50] X Li, X Zhang, W Yang, L Guo, L Huang, X Li and W Gao. Preparation and characterization of native and autoclaving-cooling treated *Pinellia ternate* starch and its impact on gut microbiota. *International Journal of Biological Macromolecules* 2021; **182**, 1351-1361.

[51] BA Alimi and TS Workneh. Structural and physicochemical properties of heat moisture treated and citric acid modified acha and iburu starches. *Food Hydrocolloids* 2018; **81**, 449-455.

[52] H Gu, H Yao and F Wang. Structural and physicochemical properties of resistant starch from Chinese chestnut (*Castanea mollissima*) prepared by autoclaving treatment and pullulanase hydrolysis. *Journal of Food Processing and Preservation* 2018; **42(1)**, e13364.

[53] H Li, R Wang, J Liu, Q Zhang, G Li, Y Shan and S Ding. Effects of heat-moisture and acid treatments on the structural, physicochemical, and *in vitro* digestibility properties of lily starch. *International Journal of Biological Macromolecules* 2020; **148**, 956-968.

[54] SI Rafiq, S Singh and DC Saxena. Effect of heat-moisture and acid treatment on physicochemical, pasting, thermal and morphological properties of horse chestnut (*Aesculus indica*) starch. *Food Hydrocolloids* 2016; **57**, 103-113.

[55] RHB Setiarto, HD Kusumaningrum, BSL Jenie, T Khusniati, N Widhyastuti and I Ramadhani. Microstructure and physicochemical characteristics of modified taro starch after annealing, autoclaving-cooling and heat moisture treatment. *Food Research* 2020; **4(4)**, 1226-1233.

[56] C Zhang, M Qiu, T Wang, L Luo, W Xu, J Wu, F Zhao, K Liu, Y Zhang and X Wang. Preparation, structure characterization, and specific gut microbiota properties related to anti-hyperlipidemic action of type 3 resistant starch from *Canna edulis*. *Food Chemistry* 2021; **351**, 129340.

[54] A Chakravarty, M Tandon, S Attri, D Sharma, P Raigond and G Goel. Structural characteristics and prebiotic activities of resistant starch from *Solanum tuberosum*: Kufri Bahar, a popular Indian tuber variety. *LWT* 2021; **145**, 111445.

[58] KO Falade and OE Ayetigbo. Effects of annealing, acid hydrolysis and citric acid modifications on physical and functional properties of starches from four yam (*Dioscorea spp*.) cultivars. *Food Hydrocolloids* 2015; **43**, 529-539.

[59] PC Martins, LC Gutkoski and VG Martins. Impact of acid hydrolysis and esterification process in rice and potato starch properties. *International Journal of Biological Macromolecules* 2018; **120**, 959-965.

[60] D Qiao, L Yu, H Liu, W Zou, F Xie, G Simon, E Petinakis, Z Shen and L Chen. Insights into the hierarchical structure and digestion rate of alkali-modulated starches with different amylose contents. *Carbohydrate Polymers* 2016; **144**, 271-281.

[61] X Wang, CK Reddy and B Xu. A systematic comparative study on morphological, crystallinity, pasting, thermal and functional characteristics of starches resources utilized in China. *Food Chemistry* 2018; **259**, 81-88.

[62] D Zhou, Z Ma, J Xu, X Li and X Hu. Resistant starch isolated from enzymatic, physical, and acid treated pea starch: Preparation, structural characteristics, and *in vitro* bile acid capacity. *LWT* 2019; **116**, 108541.

[63] Y Ding, J Huang, N Zhang, SK Rasmussen, D Wu and X Shu. Physiochemical properties of rice with contrasting resistant starch content. *Journal of Cereal Science* 2019; **89**, 102815.

[64] SY Lee, KY Lee and HG Lee. Effect of different pH conditions on the *in vitro* digestibility and physicochemical properties of citric acid-treated potato starch. *International Journal of Biological Macromolecules* 2018; **107**, 1235-1241.

[65] Z Ma, X Yin, X Hu, X Li, L Liu and JI Boye. Structural characterization of resistant starch isolated from Laird lentils (*Lens culinaris*) seeds subjected to different processing treatments. *Food Chemistry* 2018; **263**, 163-170.

[66] W Gao, P Liu, J Zhu, H Hou, X Li and B Cui. Physicochemical properties of corn starch affected by the separation of granule shells. *International Journal of Biological Macromolecules* 2020; **164**, 242-252.

[67] Z Ma, X Yin, D Chang, X Hu and JI Boye. Long- and short-range structural characteristics of pea starch modified by autoclaving, α-amylolysis, and pullulanase debranching. *International Journal of Biological Macromolecules* 2018; **120**, 650-656.

[68] CK Reddy, S Haripriya, AN Mohamed and M Suriya. Preparation and characterization of resistant starch III from elephant foot yam (*Amorphophallus paeonifolius*) starch. *Food Chemistry* 2014; **155**, 38-44.

[69] BA Acevedo, M Villanueva, MG Chaves, MV Avanza and F Ronda. Starch enzymatic hydrolysis, structural, thermal and rheological properties of pigeon pea (*Cajanus cajan*) and dolichos bean (*Dolichos lab-lab*) legume starches. *International Journal of Food Science & Technology* 2020; **55(2)**, 712-719.

[70] Y Huo, B Zhang, M Niu, C Jia, S Zhao, Q Huang and H Du. An insight into the multi-scale structures and pasting behaviors of starch following citric acid treatment. *International Journal of Biological Macromolecules* 2018; **116**, 793-800.

[71] C Wu, R Sun, Q Zhang and G Zhong. Synthesis and characterization of citric acid esterified canna starch (RS4) by semi-dry method using vacuum-microwave-infrared assistance. *Carbohydrate Polymers* 2020; **250**, 116985.